Density Functional Study of Intramolecular Proton Transfer Mechanisms in Dithienylethylene-based Molecular Switches

Zhifei ZHU [1, 2, 3], Huirong HUANG [3], Binxin LIU [3], Qian WANG [1, 3], Jing HUANG [1, 2] *

[1] *Fujian Provincial Key Laboratory of Ecological Impacts and Treatment Technologies for Emerging Contaminants, College of Environmental and Biological Engineering, Putian University, Putian, Fujian 351100, China*
[2] *Key Laboratory of Ecological Environment and Information, Putian University, Putian, Fujian 351100, China*
[3] *Fujian Zhixin Environmental Technology Co Ltd, Putian 351100, China*

http://doi.org/10.5755/j02.ms.44086

Received 18 January 2026; accepted 20 February 2026

Dithienylethylene (DTE)-based photochromic dyes are highly valued for their thermal stability and fatigue resistance. However, conventional switching systems necessitate the utilization of UV light, which is known to be harmful to human health. Recent experiments suggest that the switching of DTE derivatives is realized by visible-light ground-state intramolecular proton transfer (IPT) rather than standard ultraviolet (UV) excited-state intramolecular proton transfer (ESIPT). The present study utilizes density functional theory (DFT) to investigate these pathways. The calculated Franck–Condon excitation wavelengths for the OH and NH configurations align with the experimental data, thereby validating the computational level of theory. Upon the transition from S_0 to S_1, the distance between C1 and C2 increases from 1.55 Å to 1.58 Å, whereas the bond remains intact. We identify a dual-pathway mechanism. The first process is a ground-state intramolecular proton transfer (GSIPT) process ($S_0 \rightarrow TS0 \rightarrow S'_0$) with a low energy barrier of 3.4 kcal/mol, which can be driven by red or infrared light (800 nm). The second process is an excitation-state intramolecular proton transfer (ESIPT) process ($S_0 \rightarrow S_1 \rightarrow TS1 \rightarrow S'_1 \rightarrow S'_0$), where the rate-determining excitation step requires 367 nm UV light. This theoretical framework elucidates the mechanism by which visible light initiates C1–C2 bond opening via IPT, thereby establishing a foundational principle for the design of all-visible-light-driven sensors for environmental monitoring.
Keywords: dithienylethylene, ground-state intramolecular proton transfer (GSIPT), excited-state intramolecular proton transfer (ESIPT), transition state, visible-light switching.

1. INTRODUCTION

Organic photochromic materials have emerged as a promising class of novel all-photon storage materials because of their excellent photostability, thermal stability, and fatigue resistance [1]. These molecules achieve binary (0,1) information storage through reversible photochemical reactions, leveraging the spectral differences between two isomers. They offer advantages such as high capacity and fast response rates. Among the numerous systems, diarylethylene, a typical P-type photochromic material [2], exhibits significant changes in polarity, conformation, and spectral properties during its light-induced reversible transformation. When coupled with fluorescent signals, the color-changing unit facilitates the construction of highly sensitive, high-resolution, and fast-response smart systems, which hold significant value in chemical sensing, optical anticounterfeiting, cell imaging, and superresolution imaging. Dithienylethylene (DTE), a diarylethene derivative in which benzene rings are substituted with thiophene units (Fig. 1a), is superior to other heterocyclic analogs in terms of photophysical properties, quantum yields, and synthetic accessibility [3 – 7]. The photochromic behavior exhibited by conventional DTE systems is derived from a 6π-electrocyclization reaction of the hexatriene backbone. After UV irradiation, the open-ring isomer undergoes conrotatory cyclization to form the closed-ring isomer. This closed-ring isomer subsequently reverts to the open form upon exposure to visible light. However, the ring-closing step in standard DTE systems typically necessitates high-energy UV light in the 300 – 400 nm wavelength range. UV radiation results in suboptimal tissue penetration and the potential to induce photodamage, thereby resulting in critical limitations for biomedical and deep-material applications [8, 9]. While molecular engineering strategies (e.g., extending π-conjugation or introducing electron-donating groups) have led to a partial redshift in absorption, these approaches frequently compromise the switching efficiency or fatigue resistance. Moreover, they lack universal design principles for fully visible-light-operated systems.

Intramolecular proton transfer (IPT) is a distinct switching mechanism that is distinct from electrocyclization. In hydrogen-bonded systems such as salicylidene aniline, active hydrogen exists in dynamic equilibrium between the proton donor (O–H) and acceptor (N) sites [10, 11]. Upon photoexcitation, excited-state intramolecular proton transfer (ESIPT) occurs when the proton migrates from oxygen to nitrogen, thereby converting the OH configuration to the NH tautomer (Fig. 1 b and Fig. 1 c).

* Corresponding author: J. Huang
E-mail: *jinghuang@ptu.edu.cn*

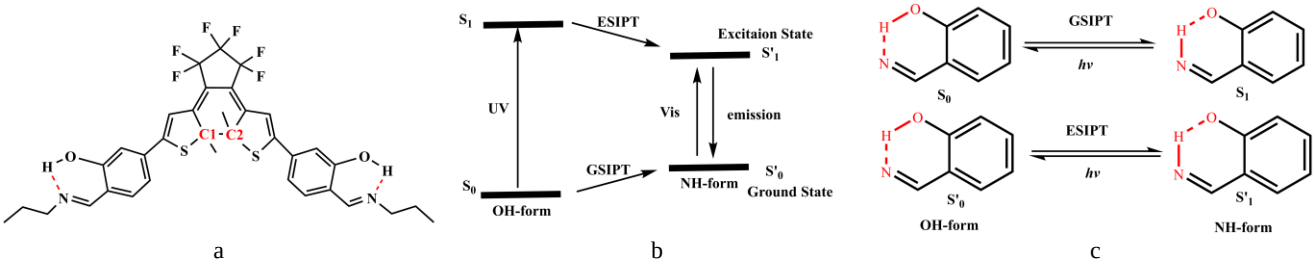

Fig. 1. a – chemical structure of the hydroxyl-imine-substituted dithienylethylene (DTE) derivative investigated in this study. The intramolecular O–H··N hydrogen bond (dashed line) and the central C1–C2 bond subject to cleavage are highlighted; b – photoinduced switching pathway from the ground-state OH configuration (S_0) to the excited-state NH configuration (S'_1); c – schematic illustration of ground-state intramolecular proton transfer (GSIPT) and excited-state intramolecular proton transfer (ESIPT) processes in the DTE system

Zhu et al. demonstrated that ESIPT-generated NH configurations exhibit significantly redshifted absorption, enabling visible-light-driven photochromism with high efficiency and stability [12, 13]. This strategy provides a molecular design blueprint for visible-light-controlled photonic switches that circumvent UV limitations [14].

The present study investigated a hydroxyl-imine-functionalized DTE derivative that operates via a dual-pathway proton transfer mechanism. Using density functional theory (DFT) and time-dependent DFT (TD-DFT), we delineate two discrete switching pathways. The first process is ground-state intramolecular proton transfer (GSIPT), which occurs after visible-light-induced structural changes. The second process is conventional ESIPT, which is initiated by UV excitation. A critical distinction between our system and previously reported ESIPT-DTE hybrids [12, 13] is the direct proton transfer that triggers C1–C2 σ-bond cleavage, as opposed to mere modulation of the absorption spectra. This enables a bond-breaking switching mechanism under mild visible/NIR irradiation. Quantum chemical calculations elucidate the geometric evolution, energy landscapes, and electronic structure changes during both pathways, thereby establishing a theoretical foundation for designing visible-light-responsive molecular switches applicable to environmental monitoring.

2. METHODS

2.1. GSIPT/ESIPT process calculations

All quantum chemical calculations were executed via the Gaussian 09 software package. Density functional theory (DFT) at the B3LYP/6-31+G(d,p) level was employed to optimize the ground-state configurations of OH (S_0), NH (S'_0), and the intramolecular proton transfer transition state (TS0). In addition, time-dependent density functional theory (TD-DFT) was utilized at the TD-B3LYP/6-31+G(d,p) level to optimize the configurations of the first singlet excited states (S_1, S'_1) and the excited-state proton transfer transition state (TS1). The polarization continuum model (IEFPCM) was incorporated to simulate the methanol solvent environment. According to the findings of previous studies, the combination of the B3LYP functional with the 6-31+G(d,p) basis set has been demonstrated to provide optimal accuracy and reliability in the description of the geometric structures of organic molecules [20 – 24]. The validity of the optimized configurations was confirmed through frequency analysis, which revealed the absence of imaginary frequencies at stable points and the presence of a single imaginary frequency in the transition state (TS) representing the proton transfer pathway. Additionally, the connectivity between the transition state and the reactants/products was confirmed via intrinsic reaction coordinate (IRC) analysis.

2.2. Energy profile calculations

To obtain more precise energy level distributions, single-point energy calculations for the ground and excited states were performed at the CAM-B3LYP/6-31++G(d,p) level with long-range correction. These calculations were based on the optimized structures described above. The solvation environment was meticulously maintained throughout the experiment. The implementation of the CAM-B3LYP functional has been demonstrated to offer a more efficacious description of the intramolecular charge transfer characteristics and excited-state energy level evolution. The objective of this study was to elucidate the photochemical response mechanism of diethynylthiophenes under visible light. To this end, we have organized energy data for reactants, transition states, and products during the ESIPT process and plotted potential energy surface level diagrams. This theoretical framework, which includes both quantum chemical and experimental components, offers a comprehensive explanation of the photochemical response mechanism and provides theoretical criteria for experimental design.

3. RESULTS AND DISCUSSION

3.1. Geometric structure optimization

The geometric parameters of the ground-state (S_0) and excited-state (S_1) structures provide critical insights into the proton transfer mechanism. As illustrated in Fig. 2, during the ground-state photomolecular proton transfer (GSIPT) process, the C1–C2 distance in the OH-configured S_0 state structure is 1.55 Å, with the intermediate six-membered ring in a closed state. For both the left and right side chains of the S_0 structure, the O-H distance is 1.01 Å, whereas the N-H distance is 1.66 Å. This indicates a stable OH··N hydrogen-bonding configuration. Upon visible-light absorption ($S_0 \rightarrow S_1$ transition), the C1–C2 distance increases to 1.58 Å while maintaining bond integrity, indicating that photoexcitation alone does not cleave the central bond. This

observation is consistent with the structural stability requirements discussed by Myles et al. [25], where maintaining specific bonding frameworks during electronic transitions is crucial for multi-addressable photochromic hybrids.

During the process of GSIPT ($S_0 \rightarrow TS0 \rightarrow S'_0$), proton migration from O to N coincides with the rupture of C1–C2 bonds. At transition state TS0, the distance between carbon atoms C1 and C2 increases to 3.71 Å, and the molecular arms deviate from coplanarity. The product S'0 (NH configuration) maintains this elongated C1–C2 distance (3.71 Å), confirming complete bond cleavage. This switching mechanism, which involves bond breaking, differs fundamentally from conventional DTE systems that rely solely on 6π-electrocyclization without σ-bond rupture [26]. Proton transfer directly drives mechanical motion (ring opening), analogous to the molecular machines described by Zhang et al. for elastronic applications [27].

As illustrated in Fig. 3, the ESIPT pathway ($S_1 \rightarrow TS1 \rightarrow S'_1$) is represented. UV excitation to the Franck–Condon state S^*_0 is followed by rapid relaxation, yielding the relaxed S_1 state. In this state, the O–H bond elongates to 1.78 Å, and the H–H distance decreases to 1.04 Å. This results in the formation of an incipient N–H bond. Proton transfer through TS1 (C1–C2 = 3.71 Å) produces S'_1 with a fully formed N–H bond (1.01 Å) and a cleaved C1–C2 bond (3.71 Å). Subsequent radiative decay to S'_0 completes the switching cycle.

3.2. GSIPT/ESIPT reaction pathways

As illustrated in Fig. 4, the energy landscape for the complete reaction process is delineated. The Frank-Condon excitation wavelength for the $S_0 \rightarrow S^*_0$ transition (OH configuration) was calculated to be 367 nm, which is consistent with the experimental value of approximately 398 nm. Furthermore, the emission wavelength of the S'1 state (NH configuration) is 593 nm, which corresponds to the experimental observation at 600 nm. According to the principles of thermodynamics, the closed-ring OH configuration (S_0) is determined to be more stable than the open-ring NH configuration (S'_0) by 8.7 kcal/mol.

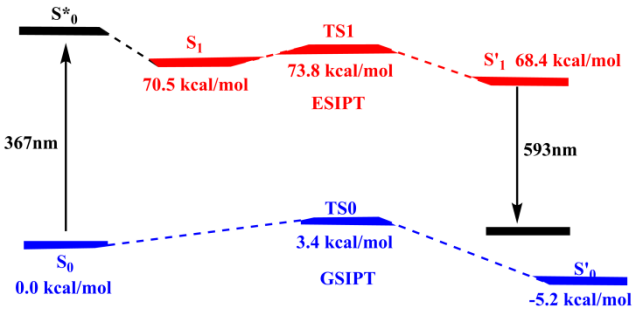

Fig. 4. Potential energy surface for ground-state intramolecular proton transfer (GSIPT, blue pathway) and excited-state intramolecular proton transfer (ESIPT, red pathway) in the dithienylethylene system. Energies are relative to S_0 in kcal/mol. The wavelength requirements for each photochemical step are indicated

The energy barriers for proton transfer are remarkably low, with values of 3.4 kcal/mol for GSIPT ($S_0 \rightarrow TS0$) and 3.2 kcal/mol for ESIPT ($S_1 \rightarrow TS1$). These low barriers enable the GSIPT pathway to proceed under thermal energy after visible-light-induced structural preorganization ($S_0 \rightarrow S_1$), requiring only red/NIR light (≥ 800 nm) for the initial excitation. In contrast, the complete ESIPT-initiated cycle ($S_0 \rightarrow S^*_0 \rightarrow S_1 \rightarrow TS1 \rightarrow S'_1 \rightarrow S'_0$) has $S_0 \rightarrow S^*_0$ excitation as its rate-determining step, necessitating UV light at 367 nm. This dual-pathway mechanism explains experimental observations: visible light triggers molecular switching via GSIPT with C1–C2 bond opening, whereas UV excitation follows a distinct pathway involving direct electrocyclization without proton transfer mediation.

The distinguishing characteristic of our system is the direct coupling between proton transfer and σ-bond cleavage under visible/NIR irradiation, a mechanism that is distinct from that of prior ESIPT-DTE hybrids, where proton transfer merely modulates absorption without bond rupture [12, 13, 28]. While microwave-assisted C–C bond formation [29] or supramolecular assemblies [30,31] have been explored for bond activation, the present work demonstrates a precise, light-controlled intramolecular proton transfer pathway that triggers bond cleavage without high-energy UV radiation.

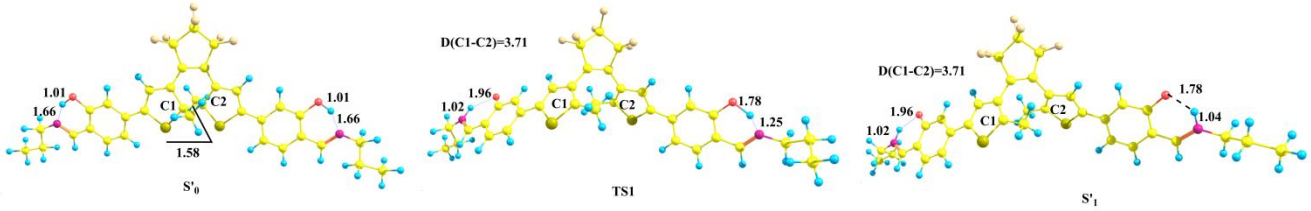

Fig. 2. Optimized geometries and key bond distances (Å) along the ground-state intramolecular proton transfer (GSIPT) pathway: S_0 (OH configuration) → TS0 → S'_0 (NH configuration).

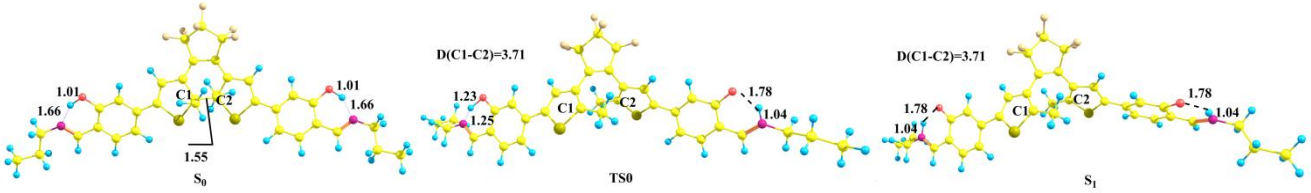

Fig. 3. Optimized geometries and key bond distances (Å) along the excited-state intramolecular proton transfer (ESIPT) pathway: S_1 → TS1 → S'_1. Proton migration coincides with C1–C2 bond rupture at the transition state

3.3. Frontier molecular orbitals

As illustrated in Fig. 5, the figure displays the HOMO and LUMO distributions for the proton transfer transition states TS0 (GSIPT) and TS1 (ESIPT). A comparison of the two transition states reveals that they exhibit analogous orbital characteristics. Specifically, the HOMO is localized predominantly on the left thiophene-benzene arm, while the LUMO concentrates on the left thiophene unit and the adjacent ethylene bridge. Negligible electron density is observed on the right molecular arm or the central C1–C2 region in either orbital. This asymmetric electron distribution indicates that photoexcitation leads to the formation of a charge-separated state, which in turn weakens the C1–C2 bond, thereby facilitating its cleavage during proton transfer. While HOMO/LUMO analysis alone cannot prove bond rupture causality, the orbital asymmetry supports a mechanism in which electronic redistribution precedes and enables proton-coupled bond cleavage.

4. CONCLUSIONS

This work elucidates a dual-pathway proton transfer mechanism in a hydroxyl-imine-functionalized dienylethylene derivative that enables visible-light-controlled molecular switching. Photoexcitation has been shown to elongate the central C1–C2 bond from 1.55 Å to 1.58 Å without cleavage. Subsequent proton transfer through either ground-state (GSIPT) or excited-state (ESIPT) pathways has been demonstrated to induce bond rupture at 3.71 Å. Notably, both pathways exhibit remarkably low energy barriers of 3.4 and 3.2 kcal/mol, respectively. Notably, the GSIPT pathway functions under red or near-infrared irradiation at wavelengths of 800 nm or longer. Conversely, the complete ESIPT cycle requires UV light at 367 nm for the initial excitation step. This system differs from conventional diarylethenes in that it directly couples proton migration to σ-bond cleavage, eschewing the use of electrocyclization as a primary mechanism. The low-barrier GSIPT mechanism establishes a design principle for visible-light-responsive molecular switches that avoid UV-induced photodamage. These derivatives demonstrate potential as fluorescent probes for in situ detection of water pollutants, including heavy metal ions and organic contaminants, in ecologically sensitive environments. The theoretical framework presented herein provides a foundation for the development of green, intelligent photofunctional materials with applications in environmental monitoring and sensing technologies.

Acknowledgments

This work was supported by the Fujian Science and Technology-Economy Integration Platform (Grant No. FJKX-2024XRH08), the National Undergraduate Innovation and Entrepreneurship Training Program (Grant No. 202411498001X), the Talent Startup Fund of Putian University (Grant No. 2024042), and the Putian Science and Technology Projects (Grant Nos. 2023GJGZ001, 2023GZ2001PTXY21, and 2025GJJ005), and the Fujian Provincial Project for Educational and Scientific Research by Young and Middle-aged Teachers (Grant Nos. JZ250039, JZ240054).

REFERENCES

1. **Wang, J., Yang, Y., Zhang, L., Li, Z.** Engineering Organic Photochromism with Photoactivated Phosphorescence: Multifunctional Smart Devices and Enhanced Four-channel Data Storage *Advanced Materials* 37 (30) 2025: pp. e2503074.
   https://doi.org/10.1002/adma.202503074
2. **Ai, Q., Lan, K., Li, L., Liu, Z., Hu, X.** Beyond Photochromism: Alternative Stimuli to Trigger Diarylethenes Switching *Advanced Science* 11 (48) 2024: pp. e2410524. https://doi.org/10.1002/advs.202410524
3. **Zakharov, A.V., Evsikova, E.E., Grebennikova, P.D., Krylova, M.A., Fakhrutdinov, A.N., Shirinian, V.Z.** Metal-free, Visible-light-mediated Phototransformations of Ortho-biaryl Appended Chalcones: Access to Oxathia [5] Helicenes and 1,2,3,4-tetrasubstituted Cyclobutanes *Organic & Biomolecular Chemistry* 23 (21) 2025: pp. 5182 – 5190.
   https://doi.org/10.1039/d5ob00490

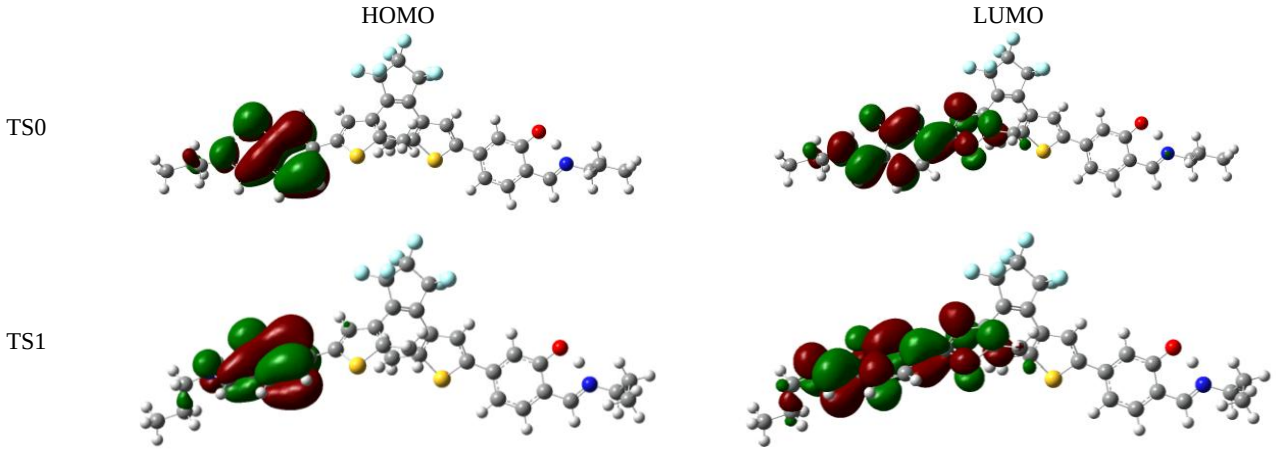

Fig. 5. Frontier molecular orbitals of transition states TS0 (GSIPT) and TS1 (ESIPT). HOMO and LUMO isosurfaces (±0.05 a.u.) exhibit asymmetric electron distributions that weaken the C1–C2 bond region during proton transfer

4. **Zhang, X., Mitchell, T.B., Benedict, J.B.** Crystal Structure Landscape of Diarylethene-based Crystalline Solids: A Comprehensive CSD Analysis *Crystal Growth & Design* 24 (15) 2024: pp. 6284 – 6291. https://doi.org/10.1021/acs.cgd.4c00556
5. **Shen, B., Ou, T., Kong, L., Song, C., Qiu, Z., Li, W., Li, R.** Synthesis and Media-dependent Photochromic Properties of Diarylindene Derivatives *ACS Omega* 10 (46) 2025: pp. 56411 – 56417. https://doi.org/10.1021/acsomega.5c08440
6. **Nishikawa, K., Ubukata, T.** Turn-on Type Ffluorescent Photochromism of a Diarylmaleimide-S,S,S',S'-tetraoxide *Photochemical & Photobiological Sciences: Official Journal of the European Photochemistry Association and the European Society for Photobiology* 24 (9) 2025: pp. 1697 – 1706. https://doi.org/10.1007/s43630-025-00774-z
7. **Guo, J., Yu, H., Jin, Y.** Synthesis and Photochromic Properties of Diarylethene Derivatives with Aggregation-Induced Emission (AIE) Behavior *Materials* 18 (11) 2025: pp. 2520. https://doi.org/10.3390/ma18112520
8. **Park, S., Ji, J., Pillai, S., Fischer, H., Rouillon, J., Benitez-Martin, C., Andréasson, J., You, J.H., Choi, J.H.** Layer-Number-dependent Photoswitchability in 2D MoS2-diarylethene hybrids *Nanoscale* 17 (6) 2025: pp. 3152 – 3159. https://doi.org/10.1039/d4nr03631j
9. **Tsujioka, T., Yamabayashi, K., Kotani, K.** Surface Glass Transition Temperature Region of Diarylethene Films Determined by Nano-marangoni Effect *Small* 20 (9) 2024: pp. e2306145. https://doi.org/10.1002/smll.202306145
10. **Yue, L., Ai, Y., Liu, Q., Mao, L., Ding, H., Fan, C., Liu, G., Pu, S.** A Novel Diarylethene-based Fluorescence Sensor for Zn2+ Detection and its Application *Spectrochimica Acta. Part A, Molecular and Biomolecular Spectroscopy* 301 2023: pp. 122960. https://doi.org/10.1016/j.saa.2023.122960
11. **Creemer, C., Kilic, H., Lee, K.S., Saracoglu, N., Parquette, J.R.** Light-controlled Self-assembly of Dithienylethene Bolaamphiphile in Water *Dalton Transactions* 2020 (20) 2020: pp. 56 – 64. https://doi.org/10.1039/d0dt02001j
12. **Hong, P., Liu, J., Qin, K.X., Tian, R., Peng, L.Y., Su, Y.S., Gan, Z., Yu, X.X., Ye, L., Zhu, M.Q., Li, C.** Towards Optical Information Recording: A Robust Visible-Light-Driven Molecular Photoswitch with the Ring-Closure Reaction Yield Exceeding 96.3 *Angewandte Chemie* 63 (8) 2024: pp. e202316706. https://doi.org/10.1002/anie.202316706
13. **Li, F., Li, M., Shi, Y., Bian, X., Lv, N., Guo, S., Wang, Y., Zhao, W., Zhu, W.H.** Single-visible-light Performed STORM Imaging with Activatable Photoswitches *Chemical Science* 16 (31) 2025: pp. 14270 – 14277. https://doi.org/10.1039/d5sc03224e
14. **Zhang, Z., Fang, H.** Regulating Excited-state Intramolecular Proton Transfer Fluorescent Property of 3-Thiolflavone by Electron Ability: Time-dependent Density Functional Theory Study *Journal of the Chinese Chemical Society* 70 (10) 2023: pp. 1854 – 1863.
15. **Hu, J., Ning, K., Fu, J., Zhou, H., Cui, S., Liu, G., Pu, S.** Construction and Applications of Photo-Controlled Fluorescent Switches Based on Diarylethene Modified Red Emission Carbon Dots *Spectrochimica Acta Part A, Molecular and Biomolecular Spectroscopy* 348 (Pt 1) 2026: pp. 127171. https://doi.org/10.1016/j.saa.2025.127171
16. **Uno, K., Nagorny, S., Aktalay, A., Kim, D., Bossi, M.L., Belov, V.N., Hell, S.W.** Fluorescent Diarylethenes with Polar Groups: Synthesis, Spectra, and Optical Microscopy Applications *Chemistry* 2025: pp. e03087. https://doi.org/10.1002/chem.202503087
17. **Fréroux, Y., Kiraev, S., Galangau, O., Phan, T.A., Roisnel, T., Maury, O., Rigaut, S., Norel, L.** Photomodulation of Dinuclear Europium (III) Complex Luminescence Using Thermally Reversible Photochromism of Diarylethene *Chemical Communications* 61 (44) 2025: pp. 8051 – 8054. https://doi.org/10.1039/d5cc01334h
18. **Yan, Q., Qiao, Z., Xu, J., Ren, J., Wang, S.** All-visible-light Triggered Photochromic Fluorescent Dithienylethene-Phenanthroimidazole: Synthesis, Crystal Structure, Multiple Switching Behavior and Information Storage. Dyes and Pigments 202 2022: pp. 110298. https://doi.org/10.1016/j.dyepig.2022.110298
19. **Qiu, S., Frawley, A.T., Leslie, K.G., Anderson, H.L.** How Do Donor and Acceptor Substituents Change the Photophysical and Photochemical Behavior of Dithienylethenes. The Search for a Water-Soluble Visible-Light Photoswitch *Chemical Science* 14 2023: pp. 9123 – 9135. https://doi.org/10.1039/D3SC01458D
20. **Huang, J., Yang, L., Zhou, Y., Chen, Y., Liu, Q., Wu, W.** Density Functional Theory/Time-Dependent Density Functional Theory Investigations on the Color-Structure Relationship of Biopigment Molecules *Journal of Chemical Research* 48 2024: pp. 1 – 7. https://doi.org/10.1177/17475198231223654
21. **Huang, J., Yang, L., Zeng, S.** Structures and Electronic Properties of Titanium Oxo Clusters with Tartrate Ligand: A Density Functional Theory Study *Materials Science-Medziagotyra* 29 (4) 2023: pp. 415 – 420. https://doi.org/10.5755/j02.ms.33426
22. **Huang, J., Yang, L., Fu, M., Chen, Z., Huang, X.** Theoretical Investigations on the Excited-State Intramolecular Proton Transfer in The Solvated 2-hydroxy-1-naphthaldehyde Carbohydrazone *Open Chemistry* 20 (1) 2022: pp. 785 – 792. https://doi.org/10.1515/chem-2022-0199
23. **Huang, J., Li, Z., Yang, L., Hu, R., Shi, G.** A Comprehensive DFT/TDDFT Investigation into the Influence of Electron Acceptors on the Photophysical Properties of Ullazine-Based D-Π-A-Π-A Photosensitizers *Scientific Reports* 15 (1) 2025: pp. 3101. https://doi.org/10.1038/s41598-025-87189-z
24. **Huang, J., Lv, Y., Wu, J.** Density Functional Theory Calculations on the Solvatochromism of Covalent Organic Framework Py-TT Cluster Compounds *Proceedings of the Royal Society A: Mathematical, Physical and Engineering Sciences* 481 (2311) 2025: pp. 20240768. https://doi.org/10.1098/rspa.2024.0768
25. **Myles, A., Wigglesworth, T., Branda, N.** A Multi-addressable Photochromic 1,2-dithienylcyclopentene-phenoxynaphthacenequinone Hybrid *Advanced Materials* 15 (9) 2003: pp. 745 – 748.
26. **Boixel, J., Colombo, A., Fagnani, F., Matozzo, P., Dragonetti, C.** Intriguing Second-order NLO Switches Based on New DTE Compounds *European Journal of Inorganic Chemistry* 2022 (12) 2022: pp. e202200034.

https://doi.org/10.1002/ejic.202200034

27. **Zhang, H., Lin, F., Cheng, W., Chen, Y., Gu, N.** Hierarchically oriented jellyfish-like gold nanowires film for elastronics *Advanced Functional Materials* 33 (2) 2023: pp. 2209760. https://doi.org/10.1002/adfm.202209760
28. **Lu, J., Yan, Q., Luo, M., Ren, J., Wang, S.** Synthesis of Photoresponsive Phenanthroimidazole-based S,S-Dioxide Dithienylethefor Information Storage and Encryption *Research on Chemical Intermediates* 50 2024: pp. 1929 – 1938. https://doi.org/10.1007/s11164-024-05236-2
29. **Yamada, T., Teranishi, W., Sakurada, N., Ootori, S., Abe, Y., Matsuo, T., Morii, Y., Yoshimura, M., Yoshimura, T., Ikawa, T., Sajiki, H.** Microwave-assisted C–C Bond Formation of Diarylacetylenes and Aromatic Hydrocarbons on Carbon Beads under Continuous-Flow Conditions *Communications Chemistry* 6 2023: pp. 78. https://doi.org/10.1038/s42004-023-00880-y
30. **Wang, H.Z., Chan, M.H.Y., Chen, Z., Chen, Z.Y., Leung, M.Y., Yam, V.W.W.** Supramolecular Self-Assembly of Dinuclear Alkynylplatinum(II) Complexes Into Highly Ordered Crystalline Hexagonal Bipyramid Superstructures *Chem* 9 (12) 2023: pp. 3573 – 3587. https://doi.org/10.1016/j.chempr.2023.08.002
31. **Aryal, P., Morris, J., Adhikari, S.B., Bietsch, J., Wang, G.** Synthesis and Self-Assembling Properties of Carbohydrate- and Diarylethene-Based Photoswitchable Molecular Gelators *Molecules* 28 (17) 2023: pp. 6228. https://doi.org/10.3390/molecules28176228

4.

5.